10 Friction parameters for the design of rock slopes to withstand earthquake loading

S. R. HENCHER, BSc PhD DIC FGS, Geotechnical Control Office, Hong Kong

Experiments to investigate the friction between rock surfaces under transient loading are described and data presented for four rock types. The method used involved a vibratory test rig and the back analysis of sliding blocks of rock. Friction values obtained in this way are compared to data from inclined plane sliding and direct shear tests. It was found that :

1) the displacement of a block due to vibration loading was greater than would have been predicted using peak friction angles obtained from static tests;

2) the apparent shear strength of the surfaces at the commencement of sliding was higher than the equivalent static strength and was dependent on the rate of loading;

3) once sliding had begun, frictional resistance reduced considerably and was several degrees lower than the equivalent static angle of friction.

The implications of these findings for slope stability analysis are considered and a finite displacement method recommended for design against earthquakes.

INTRODUCTION

1. This paper describes experiments to investigate frictional resistance developed between rock surfaces when loaded dynamically rather than statically. The results are relevant to the design of rock slopes to withstand earthquake loading.

The occurrence of rock slope failure due to vibration loading

2. Rock slope failures resulting from vibration loading commonly occur due to earthquakes and to a lesser extent blasting. As far as the author is aware there are no published back analyses of such failures that have provided values for shear strength at failure. It has, however, been demonstrated that displacements in a progressively failing slope may be related to vibration magnitude (ref.1, 2).

The design of rock slopes to withstand earthquake loading

3. The first task for design in a seismic region is to determine the magnitude and duration of forces that might affect the slope within its lifetime. Existing earthquake records and the way in which such earthquakes are related to the tectonics of the region are statistically studied and the ground motion characteristics to be included in design determined. Earthquake ground motions are however extremely complex and would be most difficult to incorporate in design. Simplifications are necessary. The most usual approach is to consider earthquake loading as a static horizontal driving force. This gross simplification has been justified because of the questionable quality of other input data in most designs (ref.3). An alternative method is to calculate the actual displacements likely to be caused in the slope due to the design earthquake (ref.4, 5, 6). The advantage of this method is that finite displacements are determined for forces that would imply total failure by using a pseudo-static force in a limit equilibrium method. The finite displacement method reflects the important transient nature of the inertial loading. It has been shown that simplifications for ease of calculation can be made by representing complex ground motions as simple acceleration pulses (ref.6).

Following such an analysis, decisions can be made on the basis of "permissable displacements" either in terms of some controlling factor of shear strength such as roughness wavelength (ref.7) or in terms of the post earthquake condition of the slope. The importance of considering the post earthquake condition is emphasised by the many reports of failures that occur days or even months following an earthquake in slopes that were previously stable (ref.8, 9).

Shear strength developed to resist transient loads

4. Whatever method is used to design a slope to withstand seismic loading, a representative shear strength must be adopted. The experiments described here were designed to investigate whether the frictional resistance developed between rock surfaces under a transient load is the same as that developed where

forces are applied more slowly as in a direct shear test. A number of observations suggest that this may not be the case :

(i) When a load is applied rapidly there may be a time lag between measured stress and strain (ref. 10). According to the adhesional theory of friction, frictional resistance is proportional to the true area of contact which varies directly with normal load. If the normal load is reduced rapidly, the area of contact may adjust more slowly resulting in a higher measured strength than if the load were reduced at a lower strain rate.

(ii) Frictional resistance is low for surfaces that have only been in contact for a short period prior to shearing (ref. 11, 12). Scholz and Engelder (ref. 12) were able to relate this time dependence to the change in real area of contact with time. In the case of a sliding block, the period of contact between any two points on the surfaces is only momentary; hence frictional resistance may be low during sliding.

(iii) Compressive strengths of many materials are dependent upon the rate of loading, higher strengths being achieved for faster rates. The shear strength of rough rock joints, particularly at high stresses, involves shearing through intact rock. One would therefore expect shear strength under rapid loading to be higher. The tests reported here were carried out on flat surfaces but loading rate dependency may be important for natural rock joints.

ROCK DESCRIPTIONS AND SAMPLE PREPARATION

5. Tests were carried out using four different rock types. Rocks were chosen on account of their homogeneity and small grain size relative to the size of the sliding surfaces. Surfaces were saw cut and then ground using a 220 grade diamond wheel.

The rock types are described briefly below :

Darleydale sandstone

6. This rock is a poorly sorted subarkose consisting mainly of angular quartz and feldspar grains of average size 0.25mm. Surfaces were scratched using minerals defining Moh's scale of hardness and examined by microscope. The main factor controlling scratching strength of the surface is the bonding of grains by pressure solution. Pores are partially infilled with iron oxides and clay minerals, possibly providing some additional strength. Many grains are fractured and are therefore weak compared to the strong intergranular bonding. Surface wear results from the fracture and rounding of embedded grains. Whole grains are not generally plucked from the surface.

Permian sandstone

7. This rock is a mature sandstone consisting of mainly quartz grains of average size 0.25mm, showing high sphericity. The rock is friable with weak bonding between grains which are generally unfractured. When the surface is scratched whole grains are removed from the surface rather than individually modified. Surface wear occurs by the progressive loosening of grains as the free surface changes. As a result this rock does not show as marked a reduction in strength with displacement nor with the removal of loose rock flour as other rock types.

Portland limestone

8. This rock is a poorly washed oobiosparite consisting largely of spherical ooliths of approximately 0.25mm diameter. The ooliths consist of clay size particles of calcium carbonate often surrounding a central nucleus. The ooliths are coalescent with secondary cementation by sparry calcite. When the surface is scratched with minerals harder than 2 on Moh's scale, asperities are smoothed and grooves cut with shiny surfaces. Fine white flour is produced.

Delabole slate

9. This rock is a fine grained metamorphic rock with a poorly developed slatey cleavage. The rock is well indurated and surface wear takes place by smoothing of the surfaces with the accumulation of very fine rock flour. Specimens were cut and ground parallel to the cleavage.

INCLINED PLANE SLIDING

10. To investigate frictional resistance under transient loading a simple test was devised using the model of a block on an inclined plane. In order that the results from the vibration tests could be compared to values obtained from more conventional 'static' tests such as direct shear, for similar ground surfaces, it was first necessary to study the frictional resistance developed by a block on an inclined plane where sliding was induced by the weight of the block alone. Variations in frictional resistance with displacement were measured for each rock type so that the effects of rate of loading in vibration tests could be distinguished. The static tests were carried out by placing a weighted thin slice of rock on a large milled surface of rock and then gradually tilting the surface by means of a screw device until sliding occurred. Each run involved approximately 160mm differential displacement and runs were repeated for up to 11.0m total displacement. Angles of sliding from inclined plane sliding tests are referred to as ϕ_{st} (ϕ_{static}).

The main conclusions from these tests are summarised as follows :

(i) The inclined plane sliding test gives repeatable results for ground surfaces of rock.

(ii) Peak angles of sliding from inclined plane tests agree well with angles of friction obtained from direct shear test data for similar ground surfaces.

(iii) Residual angles of sliding of nearly a third of peak values may be obtained by repeated sliding.

(iv) Much lower residual angles of sliding are reached for surfaces where rock flour is removed between runs rather than allowed to accumulate.

(v) Different residual angles of sliding are obtained for surfaces under similar conditions if the earlier stages of the test are conducted in a different manner.

(vi) The area of wear is controlled by the asymmetric stress distribution over the area of contact (ref. 13).

VIBRATION TESTING

Experimental method

11. A general view of the test apparatus is given in fig. 1. The test rig consisted of a tilting table to the top of which could be fixed large, milled slabs of rock, (see fig.2). This assembly was bolted onto a base plate that could slide horizontally on low friction bearings. The base plate was fixed to end plates by means of extension springs that could be adjusted to accelerate the table by 0 to 1g horizontally at frequencies of 1 to 5 Hz, where g is the acceleration due to gravity. When a locking device was released, the tilting table moved backwards and forwards in damped harmonic motion. The base acceleration was measured by an accelerometer and plotted against time by a chart recorder. The sliding block consisted of a block of steel with a thin slice of ground rock fixed to the underside. The calculations of frictional resistance relied upon measuring incremental displacements of the block accurately over a period during which the applied forces were known. To do this each test was filmed and each frame of the film examined under a microscope. Matching of the film record with the acceleration record was carried out graphically using a visual display terminal rather than on the basis of individual film frames.

Further details of the experimental method, checks on accuracy and preparation of specimens are given in ref. 14.

Calculation of frictional resistance for incremental displacements

12. Where a block sits on a slope inclined at β^{o} which is less than the angle of friction, ϕ^{o}, the block is stable. If a horizontal acceleration greater than a critical acceleration is applied to the block, directed out of the slope, displacement will occur. This is illustrated diagrammatically in fig. 3. The horizontal axes represent time.

In diagram (i) the base acceleration is given.

In diagram (ii) the inertial acceleration acting upon the block due to the base acceleration is given. The inertial acceleration is equal to the base acceleration but has a phase difference of 180°.

In diagram (iii) the shearing component of the inertial acceleration is added to the down slope gravitational acceleration acting on the block.

In diagram (iv) the magnitude of the maximum retarding acceleration due to frictional resistance is given.

In diagram (v) the maximum retarding acceleration is superimposed on the shearing acceleration.

In diagram (vi) the velocity of the block resulting from the accelerations in diagram (v) is given and in diagram (vii) the cumulative displacement is shown.

From time t_o until t_1 the shearing acceleration exceeds the maximum retarding acceleration. The block begins to move at t_o and reaches maximum velocity at t_1.

The block begins to slow down from time t_1 as the frictional resistance exceeds the shearing force.

At time t_2, when area A = area B, (velocity = 0), the block will stop sliding.

The block will then sit stable on the slope until time t_3 when again the shearing force exceeds the frictional resistance.

In this way the displacement of a block may be calculated for a known magnitude, frequency and duration of base acceleration providing the frictional resistance is known. Conversely, if a block is seen to travel a certain distance in a time during which the applied forces are known, the frictional resistance acting for that time can be determined. Such an approach was followed in this study to investigate the effect of vibration on friction.

13. Fig. 4 illustrates the method used to calculate frictional resistance from the test data.

At times t_1, t_3 and t_5 the displacements of the block d_1, d_2 and d_3 relative to the basal surface were measured from consecutive frames of the film. Average velocities (v_1 and v_2) were calculated for intermediate times t_2 and t_4 so that :

$$v_1 = \frac{d_2 - d_1}{\Delta t} \text{ and } v_2 = \frac{d_3 - d_2}{\Delta t}$$

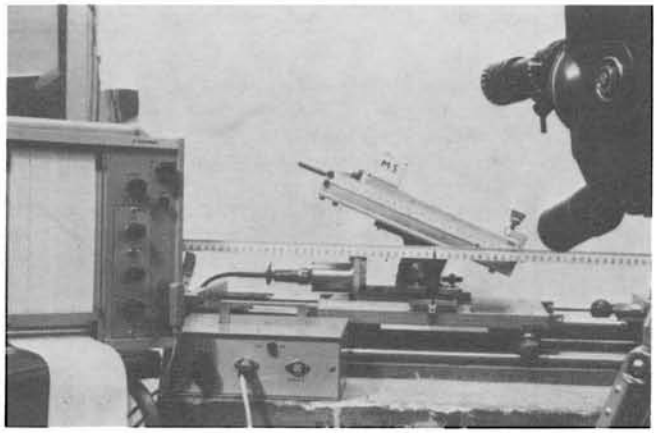

Fig. 1 General view of test apparatus

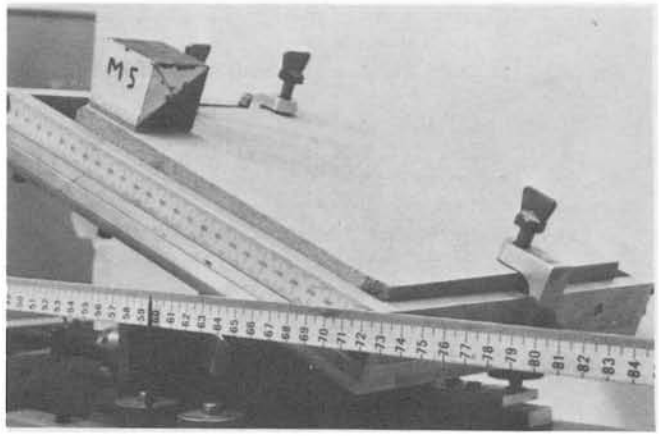

Fig. 2 Inclined plane and block

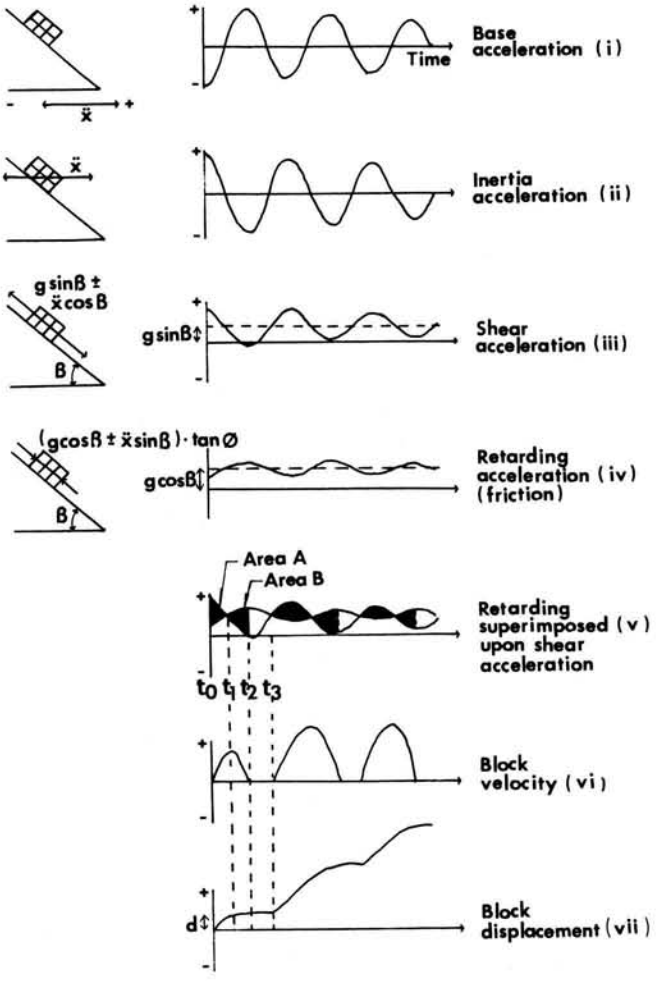

Fig. 3 Behaviour of a block on an inclined plane subjected to horizontal vibrations

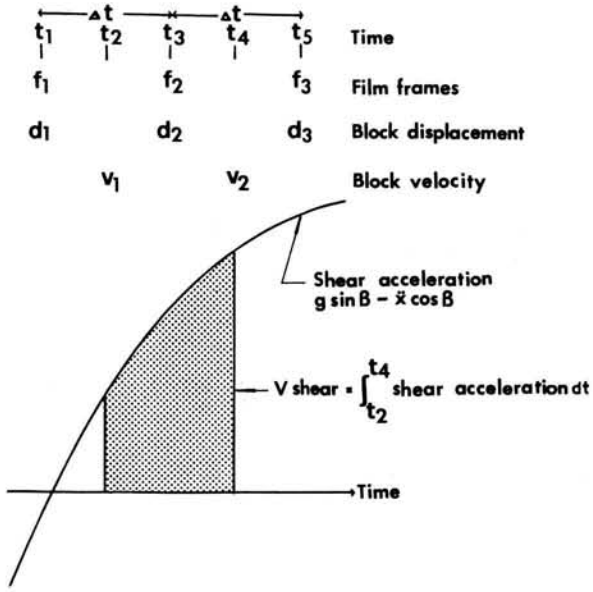

Fig. 4 Method to calculate frictional resistance for incremental displacements

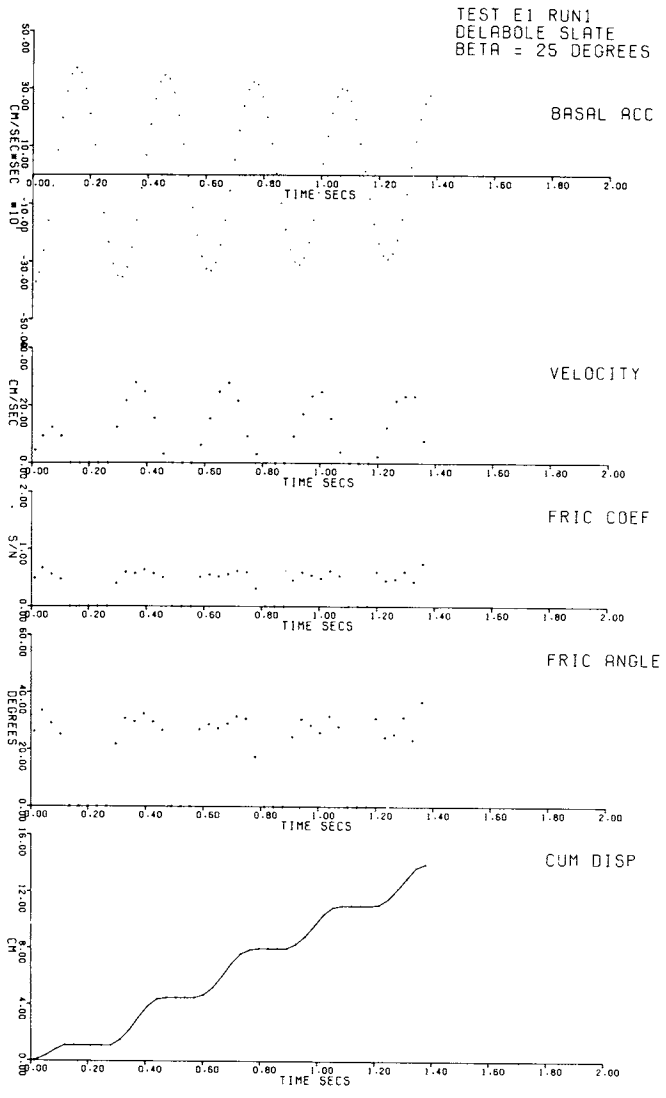

Fig. 5 Example of vibration test results

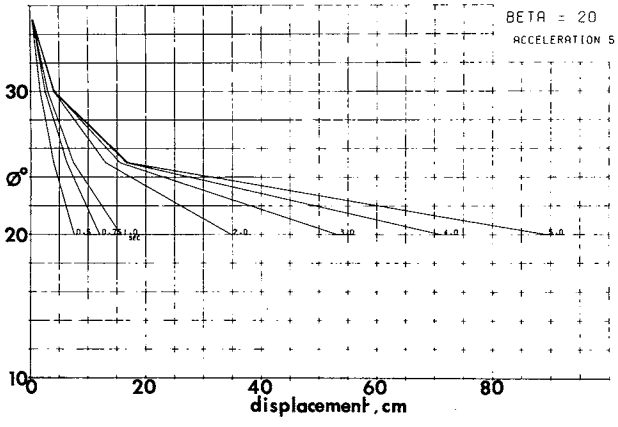

Fig. 6 Example of graph used to determine ϕ_{av}

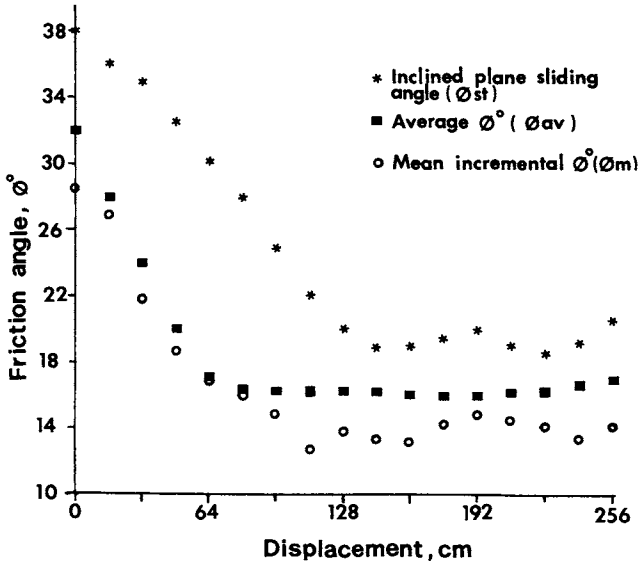

Fig. 7 Friction angles from vibration tests compared to friction angles from inclined plane sliding tests

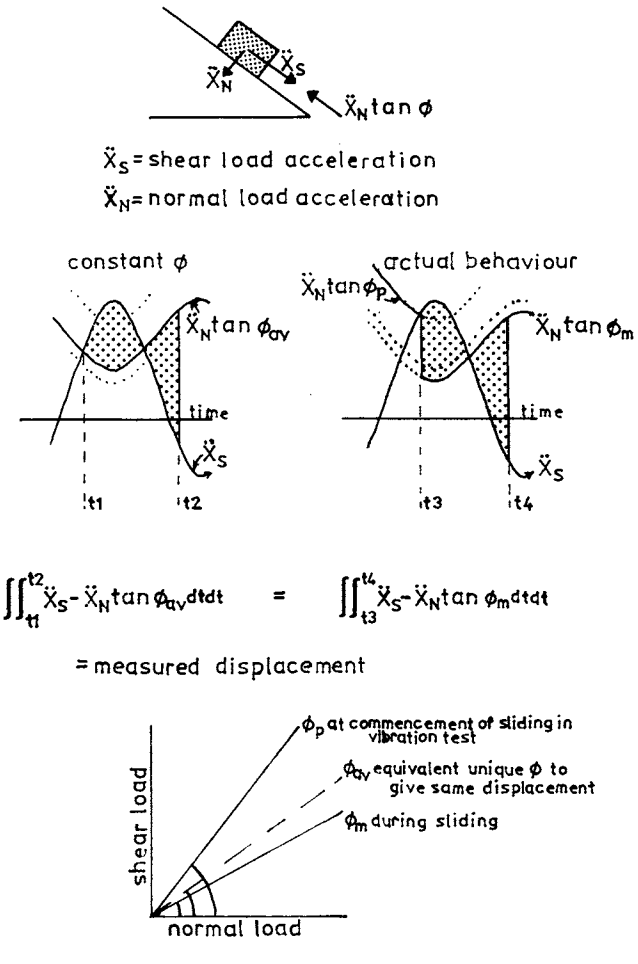

Fig. 8 Diagram to explain the difference between ϕ_m, ϕ_{av} and ϕ_p

where Δt is the time interval between film frames. Between times t_2 and t_4 the block was accelerated by a known shear load. By integrating the shear load acceleration against time for that period, the velocity (v_{shear}) ideally gained by the block can be found (disregarding friction), so that :

$$\text{for } \phi = 0^o,\ v_1 + v_{shear} = v_2$$

However friction slows the movement of the block so that :

$$v_1 + v_{shear} > v_2$$

and $v_1 + v_{shear} - v_2$ equals the integral of the deacceleration due to frictional resistance against time.

Now assuming a totally frictional material, where the frictional resistance is directly proportional to load applied normally between the surfaces, then :

$$S = \mu N$$

where S = frictional resistance
N = normal load
μ = coefficient of friction.

Referring to fig. 3,

The applied shear load acceleration is $g \sin\beta + \ddot{x} \cos\beta$

the normal load acceleration is $g \cos\beta - \ddot{x} \sin\beta$

and the deacceleration due to frictional resistance is $\mu(g \cos\beta - \ddot{x} \sin\beta)$

where $\ddot{x}$ is the inertial acceleration.

$$\text{Then } v_1 - v_2 + \int_{t_2}^{t_4} (g \sin\beta + \ddot{x} \cos\beta)\, dt = \int_{t_2}^{t_4} \mu(g \cos\beta - \ddot{x} \sin\beta)\, dt \qquad (1)$$

A typical graphical output from a program used to solve this equation for μ from test data is given in fig. 5.

Calculation of frictional resistance for larger displacements

14. Average values of ϕ, where $\mu = \tan\phi$, were determined for larger displacements of the block i.e. for individual cycles of motion and for the complete length of sliding by the following method. Theoretical displacements were calculated for different sections of each acceleration record using a range of possible values for ϕ. These calculated displacements were then compared to actual measured displacements to arrive at an average value for ϕ (ϕ_{av}).

A typical output for a single slope angle is given in fig. 6. Referring to this figure, if the block was seen to slide 15 cm in the first 2.0 sec. of the test run, the operative angle of friction would have been 24.5°. If in the first 0.5 sec. the block only slid 3 cm then the operative angle of friction would have been 26°. The average angles of friction (ϕ_{av}) obtained in this way were compared to values calculated from incremental displacements.

RESULTS

15. An example of the results obtained, based on data from individual film frames, is shown in graphical form in fig. 5. The results generally show scatter mainly due to reading errors in displacement measurements but possibly in part due to real variations in ϕ during sliding. The errors are important for incremental values of ϕ but tend to cancel out for complete runs. Results were treated statistically to give mean values from the incremental angles of friction (ϕm) and plotted as histograms and cumulative frequency curves of incremental friction values.

16. One test on Portland limestone consisted of 17 runs with the angle of slope being progressively reduced from 30° to 10° . Rock flour was removed for the first 14 runs and accumulated for the final 3. Values for ϕm (mean incremental values for ϕ), ϕ_{av} (average operative values of ϕ calculated from total displacement of the block), and ϕ_{st} (angles of sliding from inclined plane sliding tests), are plotted against displacement in fig. 7. Table 1 contains data from this test and from tests on three other rock types.

DISCUSSION

17. Fig. 7 shows that the reduction in friction with displacement in vibration tests followed the pattern observed in inclined plane sliding tests. This was also shown by tests on other rock types. The measured angle of friction was lower for the vibration tests and displacements calculated on the basis of inclined plane sliding test results would have clearly underestimated the true displacements.

18. Fig. 7 and table 1 also reveal that ϕm was generally less than ϕ_{av}. This means that although the frictional resistance during sliding was calculated at one value (ϕm), the total displacement was less than would be expected on the basis of ϕm and indicated a higher average friction angle (ϕ_{av}). This may be explained where the block commenced sliding at a later time and at a higher shear load : normal load ratio than would have been the case if strength was controlled before sliding by ϕm. Once sliding, the friction angle reduced to ϕm. This concept is illustrated in fig. 8. The times at which the block commenced sliding at the start of each displacement cycle were found by extrapolation of displacement increment data and the shear load : normal load ratios at those times calculated. Friction angles (ϕ_p) when the block began sliding in vibration tests were found to be very high and are given in table 1 together with comparable angles of sliding (ϕ_{st}) from inclined plane sliding tests. The peak angles of friction (ϕ_p) occurred at the beginning of each cycle of movement and

therefore several values of ϕ_p were obtained for each test run. It was found that the value of ϕ_p generally decreased during each test run and it is this range of values that are given in table 1.

Table 1. Friction angles from vibration tests compared to inclined plane sliding test results

Rock Type	Test No.	Run No.	Dispt. (cm)	ϕ^o_m	ϕ^o_{av}	ϕ^o_{st}	ϕ^o_p (Range)	Comments
Portland limestone	1	1	0	28.7	32.0	38.0	51/48	Rock flour removed
		2	16	27.0	27.0	35.5	51/47	
		3	32	21.9	23.0	34.5	46	
		4	48	18.8	19.0	32.5	41/40	
		5	64	16.8	17.0	30.0	33/32	
		6	80	16.0	16.3	28.0	32/28	
		7	96	14.9	16.3	25.0	31/28	
		8	112	12.8	16.3	22.0	30/27	
		9	128	14.0	16.3	20.0	31/29	
		10	144	13.5	16.3	19.0	32/28	
		11	160	13.2	16.0	19.0	28	
		12	176	14.4	16.0	19.5	30/28	
		13	192	15.0	16.0	20.0	29/28	
		14	208	14.4	16.3	19.0	29	
		15	224	14.2	16.3	18.5	30/27	Rock flour accumulated
		16	240	13.5	16.8	19.0	30/27	
		17	256	14.0	17.0	20.5	30/28	
Darleydale sandstone	1	1	0	27.9	29.0	33.0	44/41	
		2	16	25.9	27.3	28.0	43/42	
	2	1	0	26.7	29.5	33.0	38/30	
		2	16	27.7	28.0	28.0	38/32	
		3	32	27.6	27.8	27.5	38/29	
	3	1	0	28.0	30.0	33.0	39/33	
		2	16	28.1	28.8	28.0	39/33	
		3	32	27.6	28.0	27.5	39/33	
	4	1	0	25.0	28.8	33.0	40/34	
		2	16	24.3	27.5	28.0	44/37	
Permian sandstone	1	1	0	23.9	27.0	32.5	44/39	
		2	16	24.1	26.5	28.5	44/43	
	2	1	0	24.6	26.8	32.5	40/33	
		2	16	22.5	25.5	28.5	40/33	
Delabole slate	1	1	0	28.2	29.3	29.8	43/40	
		2	16	26.3	27.5	28.0	44/42	
	2	1	0	27.4	29.0	29.8	38/32	
		2	16	27.1	28.5	28.0	38/32	

Variation in peak friction angle with rate of loading

19. In table 2, peak friction angles (ϕ_p) are given for the beginning of each displacement cycle in two tests on Permian sandstone. Table 2 also gives the angle of inclination of slope (β^o), the horizontal acceleration acting on the block at time of failure ($\ddot{x}_c$) and the peak accelerations before and after commencement of sliding, ($\ddot{x}_1$ and $\ddot{x}_2$). It is clear that ϕ_p varied both with angle of slope and within each run. The decrease in ϕ_p during each run is considered not to be due to wear of the surfaces as the results from test 2 run 2 were almost identical to those for run 1 for the same surfaces. It has been shown, (ref. 14), that the rate of change of the ratio of shear load to normal load decreases both with angle of slope and with time where the horizontal basal acceleration is damped harmonic, and a clear relationship was found between this rate of change and ϕ_p (fig. 9). Peak friction angles at the beginning of each displacement cycle were higher for higher rates of change. At lower rates, ϕ_p approached the values obtained from inclined plane sliding tests ($\phi_{st} = 32^o$ for Permian sandstone). ϕ_p was never found to be lower than the equivalent ϕ_{st} from inclined plane sliding. The implication from these results is that the critical acceleration for the initiation of sliding will be higher for high frequency vibrations than for low frequency vibrations.

Table 2. Peak friction angles (ϕ_p) from Permian sandstone tests.

Test No.	Run No.	Dispt. cycle	ϕ^o_p	β^o	$\ddot{x}_c$	$\ddot{x}_1$	$\ddot{x}_2$
					cm sec^{-2}		
1	1	1	43.9	25	336	-370	359
		2	43.1		321	-348	336
		3	39.2		249	-324	313
1	2	1	43.5	25	328	-374	359
		2	40.7		275	-351	336
		3	42.6		311	-325	315
2	1	1	40.0	20	357	-371	357
		2	38.7		331	-351	331
		3	36.9		298	-325	310
		4	35.7		275	-305	290
		5	35.4		270	-282	270
		6	33.7		240	-263	249
		7	33.3		232	-244	232
2	2	1	40.0	20	359	-371	359
		2	38.8		334	-351	334
		3	36.8		296	-321	309
		4	35.6		273	-301	290
		5	33.2		230	-282	268

Values for ϕ during sliding (ϕ_m)

20. Once sliding commenced, the frictional resistance between the rock surfaces was no longer a function of the rate of loading, being fairly constant for complete runs at different inclinations. Variations in ϕ_m for repeated runs can be attributed to decreasing frictional resistance with displacement. In most tests, mean values of 'sliding' friction were less than the corresponding 'static' values for all rock types.

21. The high peak friction angles at commencement of sliding and low values during sliding can be explained by the mechanisms outlined in para. 4. The high values may reflect a delay in the reduction of area of contact with rapidly decreasing normal load and increasing shear load. The low values result from the poor bonds that can be formed as contacts are repeatedly made and broken.

CONCLUSIONS FROM VIBRATION TESTS

22. (i) The displacement of a block due to vibration loading is greater than would be predicted using friction angles obtained from 'static' tests.

(ii) The friction angle for the initiation

of sliding is higher than the equivalent 'static' friction angle and is higher for higher rates of loading.

(iii) The friction angle during sliding is lower than the 'static' friction angle.

IMPLICATIONS FOR DESIGN OF ROCK SLCPES TO WITHSTAND EARTHQUAKES

23. It is suggested that a rock slope design should be checked for seismic loading in two stages :

(i) A limit equilibrium analysis should be carried out using a pseudo-static force incorporating the peak ground acceleration expected at the site. A peak friction angle obtained from direct shear tests corrected for dilation should be used in this analysis. The use of a peak value will tend to result in conservative design as the actual frictional resistance may be much higher where the applied vibration is of high frequency.

(ii) If the limit equilibrium analysis shows that sliding will occur, then an estimate of the resulting displacement may be made by using Sarma's method (ref. 6). Peak acceleration and predominant period of ground motion are required for this calculation. Total displacements in the vibration tests would have been slightly underestimated for two rock types if residual angles of friction had been used for calculation. On the basis of the tests conducted it seems likely that the use of a friction angle 5° lower than the residual value obtained from direct shear tests will give an upper bound for the displacement. The implications of this displacement in terms of shear strength and redistribution of loads should be taken into account in deciding whether the design is acceptable or not.

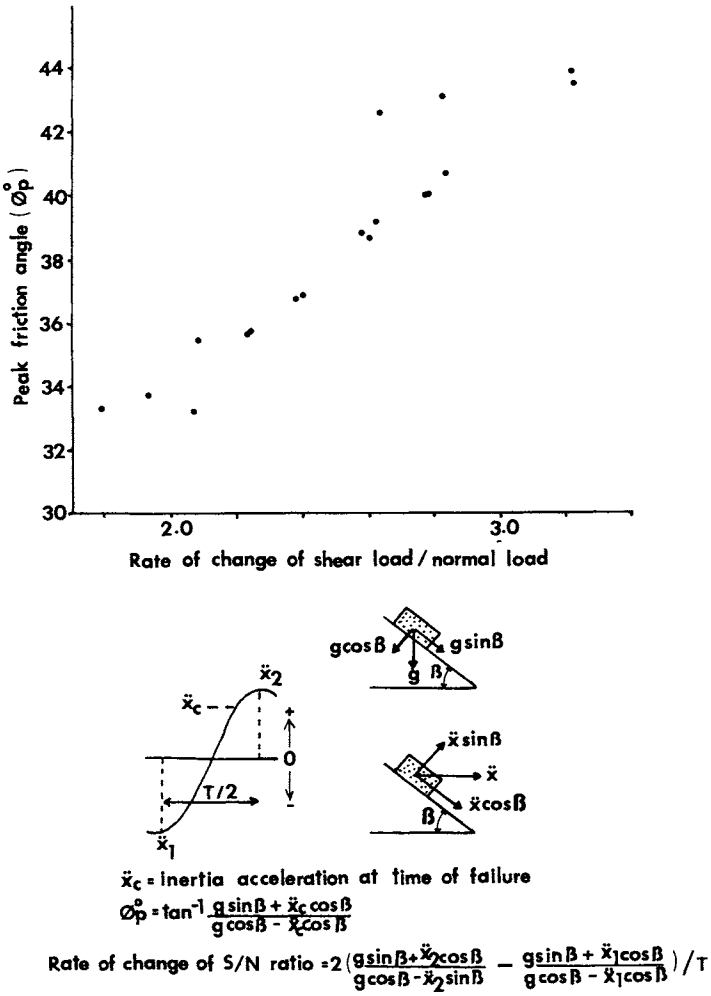

Fig. 9 Relationship between ϕ_p and rate of change of shearload : normal load ratio

24. It must be emphasised that these recommendations are based on a few experimental results using small samples with idealised surfaces. Until more information is available on the behaviour of rock slopes in earthquakes however, these recommendations seem justified.

ACKNOWLEDGEMENTS

This research was supported financially by the Natural Environment Research Council. I would like to thank Mr. M.H. de Freitas of the Engineering Geology Division, Imperial College, London for his constant encouragement and guidance, Mr. E. Rcdgers for constructing the test rig and Miss M. McKinlay and Dr. S.K.Sarma for their helpful advice. The paper was read critically by Mr. J. Bryant and Mr. A. Clover.

REFERENCES

1. ORIARD I.L. Blasting effects and their control in open pit mining. Proceedings of International Conference on Stability in Open Pit Mining, 1971, 197-222.

2. KO K.C. and McCARTER M.K. Dynamic behaviour of pit slopes in response to blasting and precipitation. Applications of Rock Mechanics. Proceedings of 15th Symposium on Rock Mechanics, South Dakota, 1973.

3. HOEK E. and BRAY J.W. Rock Slope Engineering. Institution of Mining and Metallurgy, London, 2nd Edition, 1977.

4. NEWMARK N.M. Effects of earthquakes on dams and embankments. Geotechnique, 1965, 15, No. 2, 139-160.

5. SEED H.B. A method for earthquake resistant design of earth dams. Jnl. Soil Mech. Fdn. Div. ASCE. 1966, 92, SM1, 13-40.

6. SARMA S.K. Seismic stability of earth dams and embankments. Geotechnique, 1975, 25, No. 4, 743-761.

7. HENDRON A.J., CORDING E.J. and AIYER A.K. Analytical and graphical methods for the analysis of slopes in rock masses. U.S. Army Engineers Waterways Experiment Station, NCG Technical Report No. 36.

8. U.S. GEOLOGICAL SURVEY. The San Fernando, California earthquake of February 9, 1971. U.S. Geol. Survey Prof. Paper 733, 1971.

9. CRANDELL D.R. and FAHNSTOCK R.K. Rockfalls and avalanches from Little Tahoma peak on Mount Rainier, Washington. U.S. Geol. Survey Bulletin 1221-A, 1963.

10. ROBERTSON E.C. Viscoelasticity of rocks. State of Stress in the Earth's Crust. W.R. Judd, Ed., Elsevier, New York, 1964, 181-234.

11. DIETERICH J.H. Time dependant friction in rocks. J. Geoph. Research, 1972, Vol. 77, No. 20, 3690-3697.

12. SCHOLTZ C.H. and ENGELDER J.T. The role of asperity indentation and ploughing in rock friction. Int. J. Rock Mech. Min. Sci. & Geomech. Abstr. 1976, Vol. 13, 149-154.

13. HENCHER S.R. A simple sliding apparatus for the measurement of rock joint friction, discussion. Geotechnique, 1976, No. 4, 641-644.

14. HENCHER S.R. The effect of vibration on the friction between planar rock surfaces, Ph.D. Thesis, University of London (Imperial College), 1977.